

APPLICATION OF DESIGN OPTIMISATION TO ESP PARTICLE CAPTURE

Matthew V. HORGAN^{1*} and Gary J. BROWN¹

¹Alcoa World Alumina, Kwinana, Western Australia 6966, AUSTRALIA

*Corresponding author, E-mail address: Matthew.Horgan@alcoa.com.au

ABSTRACT

Perforated plates are known to be an effective method for enhancing dust capture by Electrostatic Precipitators (ESPs). Computational Fluid Dynamics (CFD) has been used to analyse the potential benefits of perforated plates within the inlet evase of an ESP at an Alcoa refinery. Flow uniformity and dust capture were key measures of ESP performance used in this study. Axial flow uniformity was measured at discrete locations within the main body of the ESP. Particulate transport was included in the model to enable the prediction of dust capture and was implemented through use of an Algebraic Slip Model. The dust capture was modelled via a drift velocity to mimic the effect of electrostatic force and particle deposition surfaces to remove dust from the domain. The perforated plates were characterised by porosity and axial location. The performance metrics and design parameters were combined in a parametric design tool (ANSYS DesignXplorer) to efficiently identify prime design candidates. The project is effective in demonstrating the use of CFD to optimise equipment modifications, as part of a solution to a real-life, time-sensitive engineering problem.

NOMENCLATURE

A	Area
C_c	Contraction Coefficient
d_p	Particle Diameter
K	Loss Coefficient
L_s	Characteristic Length
P	Pressure
St	Stokes Number
V_s	Characteristic Velocity
W	Axial Velocity
ε	Porosity
σ_w	Standard Deviation of Axial Velocity
ρ_p	Particle Density
μ_f	Viscosity of Fluid

INTRODUCTION

Electrostatic Precipitators (ESPs) are used to remove dust from gas streams in industrial processes. Electric fields are used as the separation mechanism within the ESP, partitioning charged and uncharged phases. Highly charged corona wires within the ESP charge the passing particulate, which then moves towards grounded collector plates. The uncharged gas stream passes through the plates, unaffected by the electric fields generated by the plates. ESPs are commonly used within Alcoa alumina

refineries at the back end of the calcination stage, as a final step to remove dust from the gas being fed to the discharge stack.

The collection efficiency of ESPs is strongly dependent on achieving a uniform and low-velocity gas-flow throughout the main body of the ESP. This maximises the time available for particles to migrate to collection surfaces and minimises the likelihood of solids re-entrainment into the gas flow. The US Environmental Protection Agency (USEPA) guidelines (Parker and Plaks, 2004) suggest that standard deviation of velocity within industrial ESPs should be within 20% of the average velocity of the bulk gas stream. Similarly, industry guidelines of the Institute of Clean Air Companies (ICAC) recommend that 99% of velocities should fall within 40% of the average velocity of the bulk gas stream (Dumont and Mudry, 2003).

Haywood et al. (2006) used single-phase CFD modelling to improve the flow uniformity in ESPs at Alcoa's Kwinana refinery by optimising the spacing in a "Gas Distributor Plate" in the ESP inlet. More recently, CFD modelling at Alcoa has been used to successfully improve dust collection efficiency in ESPs through the installation of perforated plates in the ESP inlet (Figure 1).

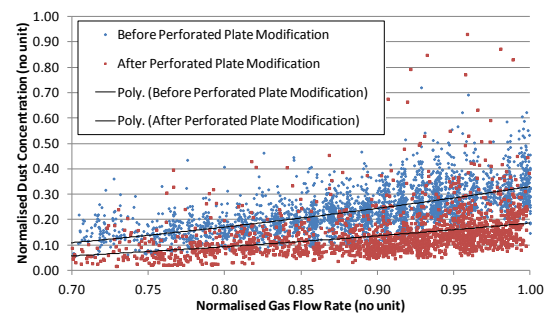


Figure 1: Improvement in dust collection after installation of perforated plate within ESP inlet. Collection improved by approximately 45% in this instance.

This paper describes the application of a multiphase CFD model and design optimisation techniques to improve the dust collection efficiency of an ESP at an Alcoa refinery, via the installation of a perforated plate within the inlet of the ESP. The standard deviation of gas velocity is used in conjunction with a direct calculation of dust concentration to measure overall ESP performance. For the purpose of this investigation, re-entrainment of dust from the hoppers back into the passing gas stream is not considered.

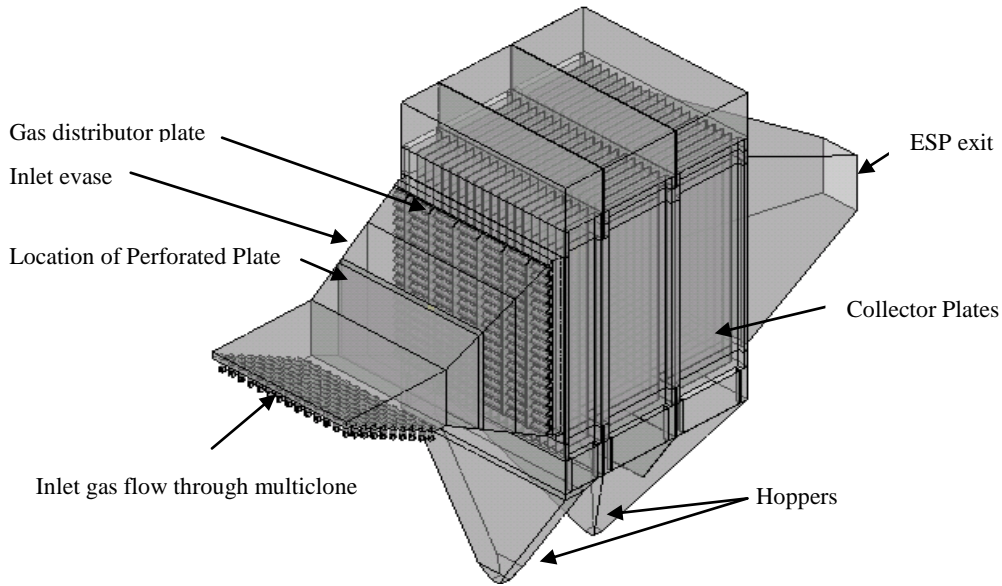


Figure 2: CFD geometry of ESP used in investigation. Gas flows through the multiclone inlet and distributor plate, before travelling through the collector plate region. Dust from the passing gas stream accumulates on these plates. The remaining gas travels through to the ESP exit.

MODEL DESCRIPTION

Geometry

The geometry of the ESP for this investigation is shown in Figure 2. Directly upstream of the ESP is a multiclone, with outlet cyclones located at the exit of this multiclone generating a swirling flow into the ESP. Gas from the multiclone then passes into the inlet evase section of the ESP. The perforated plate is located within this inlet evase section; the exact axial position of the plate being one of the two design parameters used in the optimisation study. Following the perforated plate is a gas distributor plate, used to further distribute the gas flow evenly through the ESP. Gas then flows through three banks of collector plates. Dust migrates towards, and accumulates on these plates. The remaining gas stream flows through to the exit of the ESP. Directly downstream of this is a gas stack.

Multiphase Transport Model

The Algebraic Slip Model (ASM) was selected to model the multiphase interactions between the dust and gas throughout the ESP. Selection of the ASM allows for the effects of the electric field on the dust to be modelled as a drift velocity. Throughout the rest of the ESP, the drift velocity is neglected as the local Stokes number (Eq., 1) is sufficiently low ($St \sim 5e-05$) that we consider the dust to be strongly coupled to the gas flow.

$$St = \frac{\rho_p d_p^2 V_s}{18 \mu_f L_s} \quad (1)$$

The ASM also allows the use of deposition surfaces which can be used to model the accumulation of dust on the collector plates. Particles are removed from the fluid domain when they come in contact with the deposition surfaces. Other multiphase transport models were applicable to the ESP model but not chosen, for example Eulerian-Eulerian and Lagrangian. The ASM was selected

due to the ease of implementing the local drift velocity within the collector plate region.

A common issue affecting the overall performance of ESPs is re-entrainment of dust from the hoppers back into the bulk gas stream. Re-entrainment causes dust capture to decrease and overall collection efficiency to drop. The difficulty of accurately modelling re-entrainment means that it has not been considered within this investigation. As re-entrainment has not been considered, the benefits from the perforated plate modifications are assessed using the relative changes in dust collection efficiency between design points.

Perforated Plate Loss Model

To model the perforated plate within the inlet evase, a loss model was incorporated into a porous sub-domain using a stream-wise loss coefficient. This model incorporates a source term into the momentum equations of the fluid, to account for the pressure drop across the perforated plate. As shown in Equation 2, this pressure change can be calculated based on a pressure loss coefficient. It has been assumed that viscous losses due to the perforated plate are negligible compared to inertial losses, based on work done by Haque et al. (2006).

$$\Delta P = K \frac{\rho V^2}{2} \quad (2)$$

The loss coefficient, K , is calculated using the correlation in Equation 3 (Baines and Peterson, 1951). The contraction coefficient used is 0.65, which gives the best fit to experimental data of perforated plate loss coefficients (Fried and Idelchik, 1989).

$$K = \frac{(1 - C_c \epsilon)^2}{(C_c \epsilon)^2} \quad (3)$$

The alternative to using a perforated plate model would have been to physically model the plate. This approach was not chosen due to the computational demands of a mesh with the required resolution. The perforated plate thickness of 3 mm is less than a third of the meshing sweep thickness used, while the 50 mm diameter holes would necessitate a reduction in the current face size control of 100 mm of at least 75%.

Meshing

For meshing purposes the ESP geometry was split into two regions, with the region containing the inlet evase and perforated plate being meshed separately to the rest of the ESP geometry. A generalized grid interface (GGI) was then created in the pre-processor for interpolation between the two mesh regions. Using this approach meant that only the first section containing the perforated plate was re-meshed during each optimisation step, with each change in axial plate position resulting in a change to the local mesh around the plate. There were no geometrical changes to the back-end of the ESP, so a single mesh was used for the entire optimisation process within this region.

To reduce overall meshing size, sweeps containing hexagonal elements were used where possible. To achieve this, the two ESP regions were further segregated into bodies that were either sweepable or non-sweepable. Sweepable bodies were then given swept mesh controls, and non-sweepable bodies meshed using tetrahedral elements. Where node conformance was not possible between two bodies, a GGI was used for node interpolation across the common adjoining face. Care was taken to ensure mesh element sizes were similar across each side of the interface, so that important flow characteristics were not lost.

The final mesh contained 6 million nodes and 11 million elements. Over half of these nodes were used in the meshing of the inlet multiclone and evase sections; areas containing important flow phenomena that have a large bearing on the overall ESP performance. Wall inflation was used throughout the ESP model; generally 5 layers with a smooth transition into the rest of the body mesh.

Numerical Considerations

The boundary conditions used for the ESP modelling were an inlet velocity and outlet pressure. An inlet solids concentration was also defined for the gas flow entering the ESP. These conditions were based on normal operation on site. Other flow conditions were not considered for this investigation. The SST turbulence model was chosen to model turbulence through the ESP, in addition to high resolution discretisation for the advection terms.

To model the upstream multiclone, a series of small cyclones were modelled at the inlet section of the ESP. These cyclones were used to generate the required inlet gas swirling flow. As previously mentioned, some walls were treated as deposition surfaces to facilitate the dust capture portion of the model.

Each design optimisation point was solved as a steady state problem. Numerical monitors (mass and momentum residuals) as well as physical monitors (dust and velocity values), were used to assess whether or not a steady-state

was achieved. Typically, the physical monitor points had reached a steady-state within 250 iterations, while momentum residuals in the main body of the ESP were less than 1E-04. This was considered sufficient for this model.

Design Optimisation

The ANSYS DesignXplorer tool was used in this investigation to identify the optimum plate porosity and position within the inlet evase of the ESP. As a metric of performance to compare the different design points, a calculation of dust concentration was performed at the exit of the ESP, as a direct measure of increased dust collection efficiency from the perforated plate. In addition to this, a standard deviation calculation was performed at the mid-point of the main ESP body, as detailed in Equation 4.

$$\sigma_w = \left(\frac{\sum(A_i(w_i - \bar{w}))}{\sum(A_i)} \right)^2 \quad (4)$$

This standard deviation calculation is based on the area-integral of axial velocity and is a measure of flow uniformity. The standard deviation parameter provided an effective metric to give further detail of the distribution of gas through the ESP that could be used to rank performance together with the outlet dust concentration. Finally, pressure drop was also used as a performance metric in the optimisation study. It was important that pressure drop was considered, as significant increases in pressure drop could potentially limit gas flow through the ESP.

As an initial means of choosing suitable design point permutations of plate porosity and axial position, central composite design methodology was used with Variation Inflation Factor (VIF) regression. This is an inbuilt statistical algorithm used to generate design point combinations within the local design ranges of the given input parameters. This differs to historical optimisation techniques, where combinations for every individual input parameter design point would typically be investigated.

Within this project, the DesignXplorer tool was run dynamically. Each design point resulted in an automatic change in plate position and corresponding local mesh regeneration within the inlet evase, as well as a change in porosity within the user-created plate sub-domain. Upon rebuilding the geometry and mesh for the new design point, the CFD model would then solve for the flow through the ESP before calculating and recording the three output parameters. This same procedure was carried out sequentially for each design point. Results for each design point were then added to the design of experiments. Several design points were also added later to help confirm the optimum solution, which were solved using the same method.

RESULTS

The response surface tool within the DesignXplorer application was used to analyse the different correlations between each input-output parameter combination. Analysis of sensitivity to plate position for the output parameters using 2D scatter plots (Figure 3) showed no correlation between plate position and any of the three

output metrics. Each line of best fit was close to horizontal, showing no output change for given changes in plate position. This indicates that location of the perforated plate within the inlet evase should be based on engineering considerations such as ease of accessibility and installation, rather than overall performance.

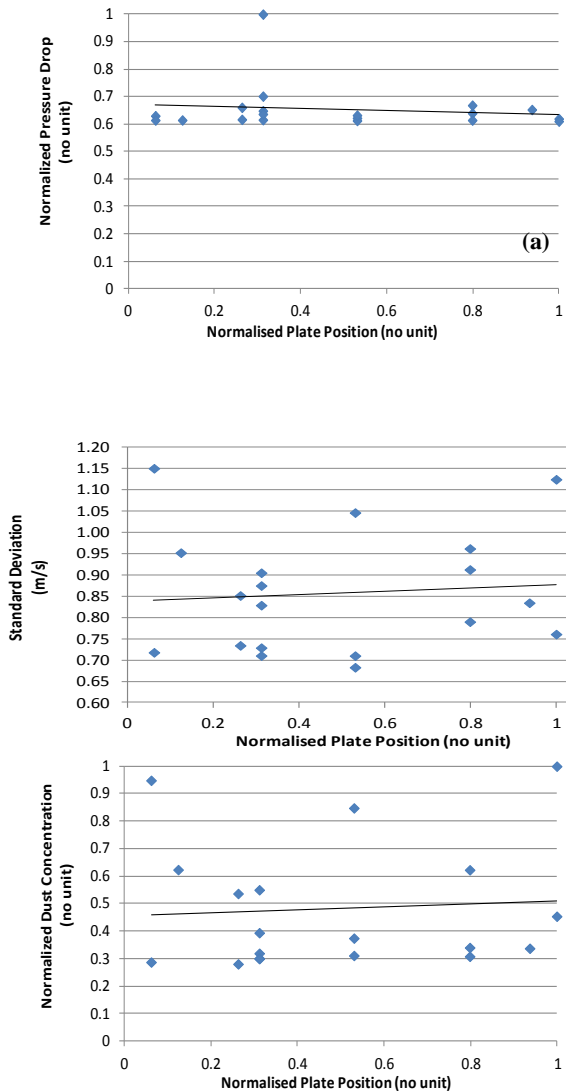


Figure 3: Response surface scatter plots of plate position vs. the three output parameters (design points are shown as \bullet), the line of best fit is shown as (—). It can be seen in (a), (b) and (c) that there is no correlation between plate position and any of the three output parameters. Each of the three lines of best fit are close to horizontal, showing no change with plate position.

Similar response surface analysis was carried out for the sensitivity of the three output parameters to plate porosity (Figure 4). It can be seen that pressure drop is inversely proportional to plate porosity (Figure 4(a)). As porosity decreases, there is a resulting increase in the overall pressure drop through the ESP which is consistent with the form of Equation 3. It can also be seen from Figure 4(a) however that the increases in pressure drop with decreasing porosity are very small within the porosity region of 0.3 to 1, with only the last point using a porosity of 0.2 resulting in a significant increase in pressure drop through the ESP. This seems to suggest that keeping the

porosity of the perforated plate above 0.3 would ensure that there are no significant detrimental impacts to gas flow through the ESP as a consequence of the plate installation.

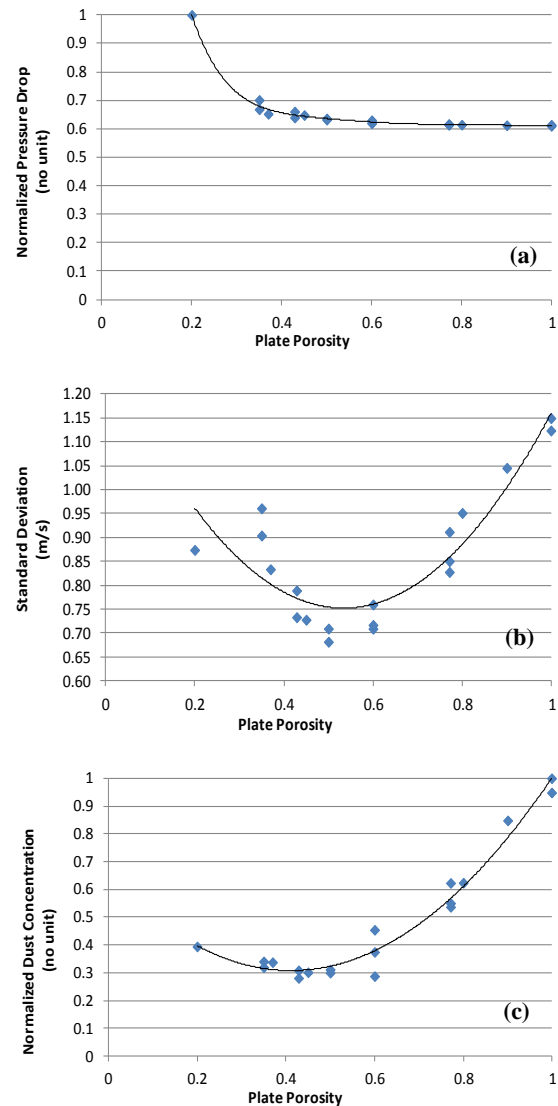


Figure 4: Response surface scatter plots of plate porosity vs. the three output parameters (design points are shown as \bullet), the line of best fit is shown as (—). Figure (a) shows pressure drop increasing with decreasing porosity. Figure (b) shows a parabolic relationship between standard deviation and plate porosity, with a minimum standard deviation correlating to a porosity of approximately 0.5. Figure (c) shows a parabolic relationship between standard deviation and plate porosity, with a minimum standard deviation correlating to a porosity in the region of 0.4 to 0.6.

Figure 4(b) shows standard deviation of gas flow decreasing with porosity down to a porosity of 0.5, before increasing again. This graph suggests that a perforated plate with porosity of 0.5 gives the most uniform gas flow through the ESP. Porosities less than 0.5 appear to have a detrimental effect on flow uniformity, with standard deviation increasing sharply with decreasing porosity below this 0.5 value. This same observation can be made for the relationship between dust concentration and plate

porosity as shown in Figure 4(c), with the minimum dust concentration at the ESP exit correlating to porosities in the region of 0.4-0.6. Although not as sharp, a similar increase in dust concentration can be seen with decreasing porosity beyond this local minimum. With higher flow uniformity meaning a more even distribution of gas across all of the collector plates, the similarities in correlations between plate porosity and each of the dust concentration and standard deviation output parameters are not unexpected.

Overall, based on the dust concentration and standard deviation output metrics, the optimum design porosity for the perforated plate is 50%. Based on the results of the CFD simulations, this porosity gives the most uniform flow through the ESP, as shown by the minimum standard deviation of axial velocity at this porosity. This correlates to the highest dust capture efficiency through the ESP, as shown by the lowest dust concentration at the exit for this porosity. Based on the results of the CFD simulations, the improvements in dust collection compared to a control case containing no perforated plate in the ESP inlet evase is approximately 53%.

Velocity contours on the centre-line of the ESP at different porosities, as illustrated in Figures 5(a) to 5(c), visually verify the optimum porosity of 0.5. It can be seen that for high porosities, such as the 0.8 porosity shown, gas flowing in from the multiclone travels along the roof of the inlet evase. This translates to a stream of high velocity gas that travels through the top section of the gas distributor plate and along the top half of the ESP, resulting in low overall flow uniformity. In contrast, a porosity that is too low, as shown by the 0.35 porosity velocity contour in Figure 5(c), forces the gas flow downwards and along the bottom of the evase, resulting in a stream of high velocity gas along the bottom of the ESP. This also results in gas flow that is highly non-uniform, highlighting the risk of using a perforated plate with a porosity that is too low. The perforated plate design of 0.5 porosity shows gas flow that is more evenly distributed along the gas distributor plate and through the ESP, correlating to high dust capture from the collector plates.

Due to time constraints, the benefit of only a single perforated plate was considered within this investigation. It is intended that further CFD analysis will be carried out to analyse the potential benefits of installing multiple perforated plates within the evase. Investigation into the benefit of perforated plates within the exit of the ESP is also intended.

CONCLUSIONS

Overall, design optimisation has been effective in helping obtain an optimum perforated plate design, within a timely manner and with minimised user input. Using an inbuilt automated optimisation tool within the CFD software, the user input required in making geometric and meshing alterations was greatly reduced. It is possible that the same conclusions could have been found using a more manual approach, however the time and user input required to do this would have been significantly greater in comparison.

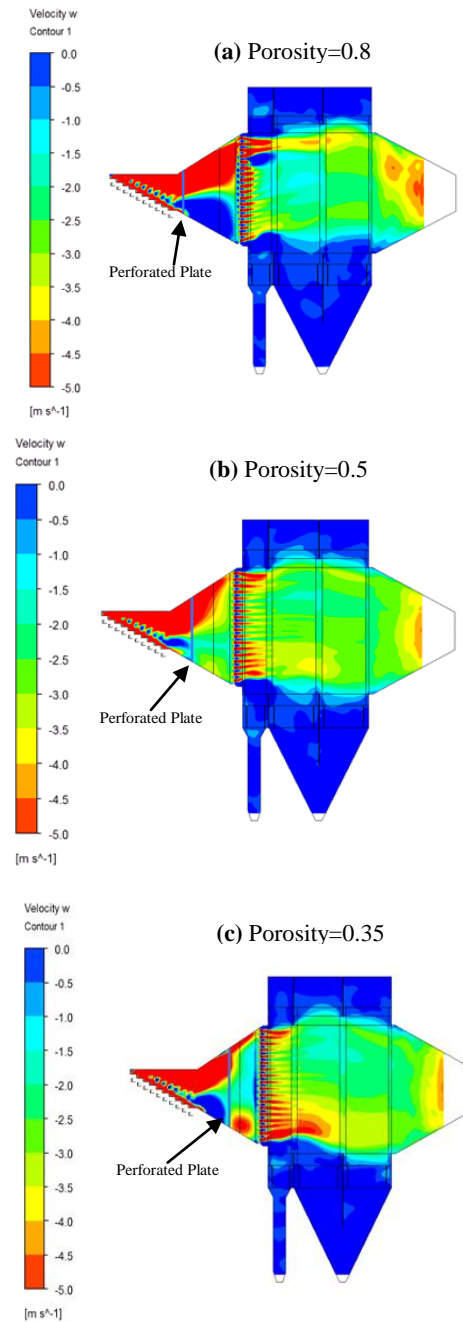


Figure 5: Velocity Contours for ESP. Plate position is different in each contour due to limited selection of design points, however as described position has no influence on output performance. Figure (a) shows that a porosity of 0.8 results in a high velocity gas stream through the top half of the ESP. Figure (b) shows that a porosity of 0.5 results in a uniform flow in the ESP. Figure (c) shows that a porosity of 0.35 results in a high velocity gas stream through the bottom half of the ESP.

Based on the CFD analysis within this investigation, it was found that ESP performance is insensitive to the position of the perforated plate within the inlet evase. The exact plate position should be based upon engineering considerations such as accessibility. Within the same analysis it was found that ESP performance is very sensitive to plate porosity. With regards to flow uniformity, dust capture and overall pressure drop, the optimum design porosity for the perforated plate is 0.5.

It is the intention of the authors that further investigation should also be made into the potential benefit of multiple perforated plates within the inlet evase and exit of the ESP. Analysis will be carried out to determine whether any improvements in dust collection efficiency from these additional plates justify the outlay to install and maintain these.

ACKNOWLEDGEMENTS

The authors would like to acknowledge the significant contribution to this study made by Dr. David Whyte and Dr. David Fletcher.

REFERENCES

BAINES, W.D. and PETERSON, E.G., (1951), "An Investigation of Flow through Screens", *Transactions of the ASME*, **73**, 467-480.

DUMONT, B.J. and MUDRY, R.G., "Computational Fluid Dynamic Modelling of Electrostatic Precipitators", *Comp. Meth. Electric Power 2003 Conference*, 5 March 2003.

FRIED, I.E. and IDELCHIK, I.E., (1989), "Flow Resistance: A Design Guide for Engineers", *Hemisphere Publishing*.

HAQUE, S.M.E., RASUL, M.G., DEEV, A., KHAN, M.M.K. and Zhou, J., "The Influence of Flow Distribution on the Performance Improvement of Electrostatic Precipitator", *ICESP X*, June 2006.

HAYWOOD, R.J., BROWN, G.J., IRONS, L.J. and STARK, M., "Using CFD to Reduce the Commissioning Time for Electrostatic Precipitators", *Proc. Fifth Int. Conf. on CFD in the Process Industries*, 13-15 December, 2006

PARKER, K. and PLAKS, N., (2004), "Electrostatic Precipitator (ESP) Training Manual", *US EPA report*, EPA-600/R-04/072.